Mechanisms of Signal Transduction:

Hsp90 Recognizes a Common Surface on Client Kinases

Ami Citri, Daniel Harari, Galit Shohat, Parameswaran Ramakrishnan, Judith Gan, Sara Lavi, Miriam Eisenstein, Adi Kimchi, David Wallach, Shmuel Pietrokovski and Yosef Yarden

J. Biol. Chem. 2006, 281:14361-14369.
doi: 10.1074/jbc.M512613200 originally published online March 21, 2006

THE JOURNAL OF BIOLOGICAL CHEMISTRY VOL. 281, NO. 20, pp. 14361–14369, May 19, 2006

Hsp90 Recognizes a Common Surface on Client Kinases*[S]

Received for publication, November 28, 2005, and in revised form, March 13, 2006 Published, JBC Papers in Press, March 21, 2006, DOI 10.1074/jbc.M512613200

Ami Citri[‡], Daniel Harari[§], Galit Shohat[¶], Parameswaran Ramakrishnan[‖], Judith Gan[‡], Sara Lavi[‡], Miriam Eisenstein[**], Adi Kimchi[¶], David Wallach[‖], Shmuel Pietrokovski[‡‡], and Yosef Yarden[‡1]

From the Departments of [‡]Biological Regulation, [¶]Molecular Genetics, [‖]Biological Chemistry, [**]Chemical Research Support, and [‡‡]Molecular Genetics, Weizmann Institute of Science, Rehovot 97100, Israel, and [§]Bioinformatics Support Unit, Ben-Gurion University of the Negev, Beer-Sheva 84105, Israel

Hsp90 is a highly abundant chaperone whose clientele includes hundreds of cellular proteins, many of which are central players in key signal transduction pathways and the majority of which are protein kinases. In light of the variety of Hsp90 clientele, the mechanism of selectivity of the chaperone toward its client proteins is a major open question. Focusing on human kinases, we have demonstrated that the chaperone recognizes a common surface in the amino-terminal lobe of kinases from diverse families, including two newly identified clients, NFκB-inducing kinase and death-associated protein kinase, and the oncoprotein HER2/ErbB-2. Surface electrostatics determine the interaction with the Hsp90 chaperone complex such that introduction of a negative charge within this region disrupts recognition. Compiling information on the Hsp90 dependence of 105 protein kinases, including 16 kinases whose relationship to Hsp90 is first examined in this study, reveals that surface features, rather than a contiguous amino acid sequence, define the capacity of the Hsp90 chaperone machine to recognize client kinases. Analyzing Hsp90 regulation of two major signaling cascades, the mitogen-activated protein kinase and phosphatidylinositol 3-kinase, leads us to propose that the selectivity of the chaperone to specific kinases is functional, namely that Hsp90 controls kinases that function as hubs integrating multiple inputs. These lessons bear significance to pharmacological attempts to target the chaperone in human pathologies, such as cancer.

Heat shock protein 90 (Hsp90)[2] is an extremely abundant chaperone (comprising ~1–2% of total cellular protein) (1) unique in the diverse but select nature of its client proteins. Hsp90 clients range from protein kinases through steroid hormone receptors and small G proteins to viral enzymes and components of the telomerase (2, 3). The breadth of Hsp90 clientele has been addressed recently in comprehensive studies in yeast (4, 5), demonstrating that roughly 10% of the yeast proteome is subject to regulation by Hsp90. The common denominator of Hsp90 clients is their essential role in the propagation of signal transduction. Because many different regulatory proteins depend on Hsp90, multiple signaling pathways are sensitive to changes in its activity (6).

Hsp90 controls the biogenesis, stability, and activity of its client proteins. The role of the chaperone in maintenance of the stability of its clients is reflected by enhanced degradation of the clients upon pharmacological inhibition of Hsp90 by ansamycin antibiotics, such as geldanamycin (GA). The function of Hsp90 during the biogenesis of client proteins (7) is such that the chaperone is essential for the maturation of the majority of its client proteins to an activation-competent state, as established early on for the Src kinase. Thus, in most cells examined, Src engages in a stable complex with the Hsp90 machinery, as long as the protein is cytosolic, but dissociates from the Hsp90-Cdc37 complex as soon as it reaches the plasma membrane (8, 9). Hsp90 is also implicated in the regulation of the signaling capacity of client proteins (10, 11). Consistently, Hsp90 has been found to interact with the effector domain of its client proteins (*e.g.* the hormone-binding domain of steroid hormone receptors and the catalytic domain of kinases). Interestingly, large variability can be found in the regulation of individual members of protein families by Hsp90. Thus, the chaperone selectively establishes a stable interaction with individual members of the family of steroid hormone receptors (3), Cyclin-dependent kinases (12), Src kinases (13), as well as ErbB family receptor tyrosine kinases (14, 15).

The interaction of Hsp90 with its client proteins is thought to be characterized by low-affinity binding and repeated cycles of association and release (16). It has been suggested that, rather than recognizing specific sequence motifs, Hsp90 interacts with features that are common to unstable proteins, such as unveiled hydrophobic patches, with a higher level of specificity being gained through the mediation of specific co-chaperones, such as the kinase-dedicated CDC37 (17). Nevertheless, the mechanism by which Hsp90 recognizes its diverse clientele remains a primary question in the field.

The specificity of Hsp90 toward its client proteins has mainly been addressed for steroid hormone receptors and kinases. In the case of the glucocorticoid receptor, a small (7-amino-acid) sequence in the amino terminus of the hormone-binding cleft was found to be crucial for recognition by Hsp90 (18). Regarding kinases, work carried out on the Lck kinase demonstrated that the amino-terminal lobe of the kinase mediates the bulk of interactions with CDC37 and Hsp90, with a major contribution associated with the hinge region between the two lobes of the kinase (19, 20).

Similar to Src family kinases, ErbB-2/HER2 is strongly coupled to Hsp90, and parallel studies have converged on a discrete region within the kinase domain of ErbB-2 that confers interactions with Hsp90 (10, 21, 22). Initial deletion analysis indicates that the kinase domain of ErbB-2 is responsible for the interaction with Hsp90 (15), whereas use of a kinase-inhibitory analog of ATP suggests that this interaction is affected by the occupation of the nucleotide-binding pocket of ErbB-2

* This work was supported by grants from the European Community, NCI, National Institutes of Health (CA72981), the Prostate Cancer Association of Israel, and the Willner Family Center for Vascular Biology. The costs of publication of this article were defrayed in part by the payment of page charges. This article must therefore be hereby marked "*advertisement*" in accordance with 18 U.S.C. Section 1734 solely to indicate this fact.

[S] The on-line version of this article (available at http://www.jbc.org) contains a supplemental table and references.

[1] Incumbent of the Harold and Zelda Goldenberg Professorial Chair in Molecular Cell Biology. To whom correspondence should be addressed: Dept. of Biological Regulation, Weizmann Institute of Science, Rehovot 97100, Israel. Tel.: 972-8-9343974; Fax: 972-8-9342488; E-mail: yosef.yarden@weizmann.ac.il.

[2] The abbreviations used are: Hsp, heat shock protein; HEK293, human embryonic kidney 293; GA, geldanamycin; 17-AAG, 17-alkylamino-17-demethoxygeldanamycin; MAPK, mitogen-activated protein kinase; MAP2K, mitogen-activated protein kinase kinase; MAP3K, mitogen-activated protein kinase kinase kinase; DAPK, death-associated protein kinase; NIK, NFκB-inducing kinase; MEK, mitogen-activated protein kinase/extracellular signal-regulated kinase kinase; MEKK, MEK kinase; ERK, extracellular signal-regulated kinase; PI3K, phosphatidylinositol 3-kinase; HA, hemagglutinin; SH, Src homology.

(14). Unlike ErbB-2, ErbB-1 interacts only weakly with Hsp90 and CDC37. Upon swapping sequences between ErbB-1 and ErbB-2, it was found that a loop connecting the αC helix to the β4 strand within the amino-terminal lobe of the kinase domain mediates the enhanced sensitivity of ErbB-2 to degradation induced by GA (21). Mutagenesis within this region demonstrated that the interactions of ErbB-2 with Hsp90 are mediated by the respective surface (22, 23) and revealed a role for Hsp90 in regulating the activity of ErbB receptors by limiting receptor heterodimerization (10).

In the present study, we have addressed the features conferring recognition of protein kinases by Hsp90. Revisiting the role of the αC–β4 loop of ErbB-2, we further established that surface electrostatics define the capacity of the kinase to be recognized by Hsp90. Applying this observation to two novel Hsp90 client kinases, NIK and DAPK, we have confirmed that their interactions with the chaperone are dependent on surface electrostatics within the αC–β4 loop. Addressing the potential to define a Hsp90 interaction motif sequence within kinase clients, we carried out a kinome-scale experimental and bioinformatic analysis of the selectivity of Hsp90 toward kinase clients and concluded that a combination of surface features, rather than a linear amino acid sequence, defines recognition by the Hsp90 chaperone. Last, addressing the functional selectivity of the Hsp90 chaperone machine, we have found that hubs within signal transduction cascades are preferred nodes of regulation by the chaperone.

EXPERIMENTAL PROCEDURES

Reagents and Plasmids—Unless otherwise indicated, materials were purchased from Sigma. GA and 17-AAG were a kind gift from Kosan Biosciences (Hayward, CA). ^{35}S-labeled cysteine and methionine was from GE-Healthcare (Buckinghamshire, UK). Anti-Hsp90 antibodies were from Stressgen (San Diego, CA), anti-HA from Babco (Basel, Switzerland), anti-epidermal growth factor receptor from Alexis (Montreal, Canada), anti-Myc from Santa Cruz Biotechnology (Santa Cruz, CA), and anti-ErbB-2 monoclonal antibodies were generated in our laboratory.

Construction of Mammalian Expression Vectors—Point mutations within the kinase domains of ErbB-1, ErbB-2, NIK, and DAPK were generated by PCR mutagenesis using the *Pfu*-Turbo enzyme (Stratagene, La Jolla, CA). An expression vector encoding HA-tagged ubiquitin was a gift from Prof. Dirk Bohmann (University of Rochester, NY).

Cell Culture and Transfection—HEK293T and COS7 cell lines were cultured in Dulbecco's modified Eagle's medium, whereas Chinese hamster ovary cells were cultured in Dulbecco's modified Eagle's medium/F-12 medium (Biological Industries, Beit-Haemek, Israel). All media were supplemented with 10% fetal calf serum (Invitrogen), 4 mM glutamine, 100 units/ml penicillin, and 0.1 mg/ml streptomycin. Transfection of HEK293T cells was performed using the calcium phosphate method. COS7 cells were transfected using JET-PEI (Qbiogene, Irvine, CA), and Chinese hamster ovary cells were transfected using Lipofectamine (Invitrogen).

Lysate Preparation, Immunoprecipitation, and Immunoblot Analyses—For analysis of protein-protein interactions, cells were lysed in solubilization buffer (50 mM sodium-HEPES, pH 7.5, 150 mM NaCl, 10% glycerol, 1% Triton X-100, 1 mM EDTA, 1 mM EGTA, 1.5 mM $MgCl_2$) containing Na_3VO_4 and a mixture of protease inhibitors. Otherwise, radioimmune precipitation assay buffer (25 mM Tris-HCl, pH 7.5, 150 mM NaCl, 0.5% sodium-deoxycholate, 1% Nonidet P-40 and 0.1% SDS0) was used. Lysates were cleared by centrifugation (10,000 × *g*, 15 min). For direct electrophoretic analysis, boiling gel sample buffer was added to cell lysates. For other experiments, lysates were first subjected to immunoprecipitation with anti-receptor monoclonal antibodies that were precoupled to rabbit anti-mouse immunoglobulin G beads by tumbling for 2 h at 4 °C. The immunoprecipitates were washed four times with the lysis buffer, resolved by SDS-PAGE through 10% gels, and electrophoretically transferred to nitrocellulose membranes. The membranes were blocked for 0.5 h in TBST buffer (0.02 M Tris-HCl, pH 7.5, 0.15 M NaCl, and 0.05% Tween 20) containing 10% low-fat milk, probed with 1 μg/ml primary antibodies for 2 h, followed by 0.5 μg/ml secondary antibody linked to horseradish peroxidase. Immunoreactive bands were detected with the ECL (enhanced chemiluminescence) reagent (Amersham Biosciences AB, Uppsala, Sweden).

Structural Analysis—The kinase domain of ErbB-2 was modeled based on the available x-ray structure of the kinase domain of ErbB-1 (Protein Data Bank (PDB) code 1M14) (24, 25). The sequence identity is 78% with no insertions/deletions. Electrostatic potential was computed with Delphi (26), as implemented in the InsightII software package (Accelrys Inc., San Diego, CA). The fractional solvent-accessible area (amino acid surface exposure) was calculated using the InsightII software package (Accelrys Inc.).

RESULTS

Hsp90 Interactions with ErbB Kinases Are Sensitive to Surface Charge within the αC–β4 Loop—We previously reported that a drug designed to covalently attach to cysteine 805 located within the kinase domain of ErbB-2 increased receptor ubiquitylation (14). The mechanism we inferred involves dissociation of Hsp90-ErbB-2 complexes, an effect observed also upon treatment with the Hsp90 inhibitor geldanamycin. Based upon the identification of a sequence motif responsible for ErbB-2 sensitivity to GA (21), we identified the αC–β4 loop of ErbB-2 as a recognition site for the Hsp90 complex (10), a finding confirmed by another group (22). In an attempt to gain further understanding of the structural basis for kinase recognition by Hsp90, we addressed the differential sensitivity of the four ErbB proteins to degradation induced by the Hsp90 inhibitor 17-AAG (Fig. 1*A*). We chose to compare the levels of endogenous kinases following treatment for short (2 and 4 h) or long (18 and 24 h) incubation periods with the drug. Degradation of ErbB-1 and -2 was addressed in COS7 cells, which express relatively high levels of ErbB-1, whereas degradation of ErbB-2, -3, and -4 was addressed in MCF7 cells, which express detectable levels of the receptors but scarcely detectable ErbB-1. Although the degradation of ErbB-1 was relatively slow, rapid degradation of ErbB-2 was observed in both cell lines. In addition, we observed slow degradation of ErbB-3 and -4, consistent with previous reports (27, 28).

Alignment of the αC–β4 loop region of ErbB-1 and -2, as well as the comparison of surface charge maps within this region from the published structure of ErbB-1 (PDB code 1M14) (25), upon which we modeled ErbB-2, revealed remarkable differences in surface charge between ErbB-1 and -2 (Fig. 1*B*). These differences are mainly attributed to a single amino acid (Asp-770 in ErbB-1 and Gly-778 in ErbB-2), which confers a significant negative charge to ErbB-1 in this region (Fig. 1*B*). The overall surface charge on the backside of the kinase domain of ErbB-1, where the αC–β4 loop is located (Fig. 1*C*), is characterized by a mainly neutral/positive surface charge, with the exception of the aspartic acid within the αC–β4 loop. Analyzing the surface exposure of residues within this loop, we found that the aspartic acid, as well as an adjacent proline, are the most highly surface-exposed residues within this sequence. Swapping glycine 778 in ErbB-2 with an aspartate (as in ErbB-1; mutant denoted G778D) stabilized the receptor toward 17-AAG-induced ubiquitylation/degradation and enhanced the kinase

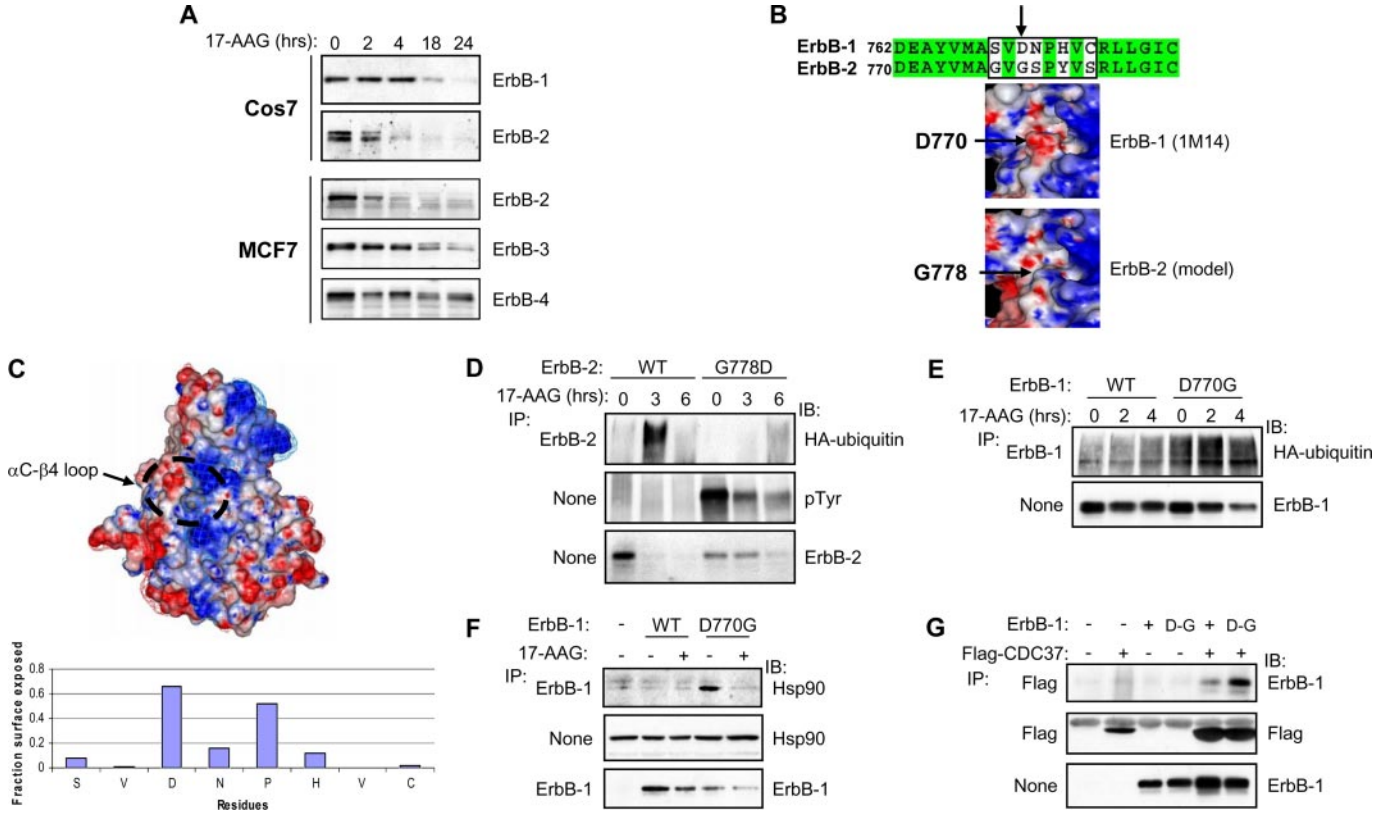

FIGURE 1. **Surface charge within the αC–β4 loop of the kinase domain of ErbB proteins governs differential regulation by Hsp90.** *A*, equally plated COS7 and MCF7 cells were treated for the indicated time intervals with 17-AAG (1 μM) followed by cell lysis, gel electrophoresis, and immunoblotting (*IB*) for the different ErbB proteins. *B*, alignment of the sequences of the αC–β4 loops of ErbB-1 and ErbB-2. The *arrow* marks the position of a divergent amino acid between the two sequences (glycine in ErbB-2 and aspartic acid in ErbB-1) (*top*). Shown are a comparison of the surface charge of the region of the αC–β4 loop (*boxed*) within the kinase domains of ErbB-1 (PDB code 1M14) and a model of the kinase domain of ErbB-2 demonstrating introduction of a surface-exposed negative charge (*red*) by the aspartic acid of ErbB-1. *C*, structure of the kinase domain of ErbB-1 demonstrating an overall neutral (*white*)/positive (*blue*) charge on the backside surface of the molecule (*top*). Shown is the fraction surface exposure of residues within the αC–β4 loop of ErbB-1 (*bottom*). COS7 (*D*) or Chinese hamster ovary cells (*E*) were transfected with expression vectors encoding HA-tagged ubiquitin, along with ErbB-2 (*D*) or ErbB-1 (*E*), either wild type (*WT*) or the indicated mutants. Twenty-four hours after transfection, the cells were subjected to treatment with 17-AAG (1 μM) followed by lysis, immunoprecipitation (*IP*) of the ErbB protein, and immunoblotting (*IB*) for HA-ubiquitin and the respective ErbB. *F*, HEK293T cells were transfected with expression vectors encoding ErbB-1, either wild type or D770G. Twenty-four hours after transfection, the cells were subjected to treatment with 17-AAG (+, 1 μM for 10 min) or left untreated (−). Following lysis, immunoprecipitation (*IP*) for ErbB-1 was carried out followed by analysis of the interactions with Hsp90. *G*, HEK293T cells were transfected with expression vectors encoding ErbB-1, either wild type or D770G (*D–G*) in the presence or absence of a plasmid encoding a FLAG-tagged CDC37. Following lysis, immunoprecipitation for FLAG-CDC37 was carried out followed by analysis of interactions with ErbB-1.

activity of the receptor dramatically, consistent with loss of regulation by Hsp90 (Fig. 1*D*) (10). The reverse mutation of aspartate to glycine on ErbB-1 (mutant denoted D770G) resulted in the opposite effect (Fig. 1*E*). In addition, D770G-ErbB-1 was found in a 17-AAG-sensitive association with Hsp90 and associated strongly with CDC37, hallmarks of Hsp90 regulation (Fig. 1, *F* and *G*). In conclusion, the surface charge in the region of the αC–β4 loop of ErbB-1, conferred by the presence of a surface-exposed aspartic acid, is a major contributing factor to the reduced dependence of ErbB-1 upon Hsp90. This conclusion is consistent with observations made by Neckers and collaborators (22).

The Novel Hsp90 Client Kinases NIK and DAPK Interact with Hsp90 through Their αC–β4 Loop—The occurrence of a specific protein fold with distinct surface features defining the differential extent of recognition of ErbB-1 and -2 by Hsp90 suggests the potential for uncovering a general Hsp90 recognition element. In line with this notion, a short motif conferring Hsp90 dependence has been previously described for the glucocorticoid receptor (18). Alignment of the motif sequences of the glucocorticoid receptor, ErbB-1, and -2 (Fig. 2*A*) demonstrates similar proline-centered hinges (19, 29). Genome-wide screens of all human proteins carried out based on this alignment did not bear statistical significance (data not shown). Therefore, we focused on kinases from different families whose sequence characteristics within the region of the αC–β4 loop were similar to those of ErbB-2. The kinases chosen were death-associated protein kinase (DAPK; CAMK family), a Ca^{2+}/calmodulin-dependent, cytoskeletal-associated protein kinase whose expression is implicated in the sensitivity of cells to apoptotic effects of tumor necrosis factor-α and interferon-γ; and NFκB-inducing kinase (NIK; MAP3K14, STE family), an essential component of the "alternative" NFκB activation pathway.

Addressing the regulation of DAPK by Hsp90, we found that degradation of endogenous DAPK was induced following inhibition of Hsp90 by 17-AAG (see supplemental table). Co-immunoprecipitation of Hsp90 demonstrated that DAPK forms a 17-AAG-sensitive complex with Hsp90 (Fig. 2*B*, *top*). When addressing the three DAPK family members, it was observed that all members (DAPK, DAPK2/ZIPK, and DAPK3/Drp1) interact with Hsp90 and undergo degradation following long periods of incubation with 17-AAG (supplemental table and data not shown). Immunoprecipitation of HA-tagged constructs of DAPK and immunoblotting for Hsp90 verified that the kinase domain of DAPK is necessary and sufficient to mediate interactions with Hsp90 (Fig. 2*B*, *bottom*). Thus, deletion of the kinase domain (mutant denoted "−KD") abolished Hsp90 interactions, whereas the kinase domain in isolation (KD) was sufficient to mediate the interaction. Examining the structure of the kinase domain of DAPK, we observed that the surface around the αC–β4 loop of the kinase is characterized by an abundance of neutral or positively charged amino acids, with similar distribution of

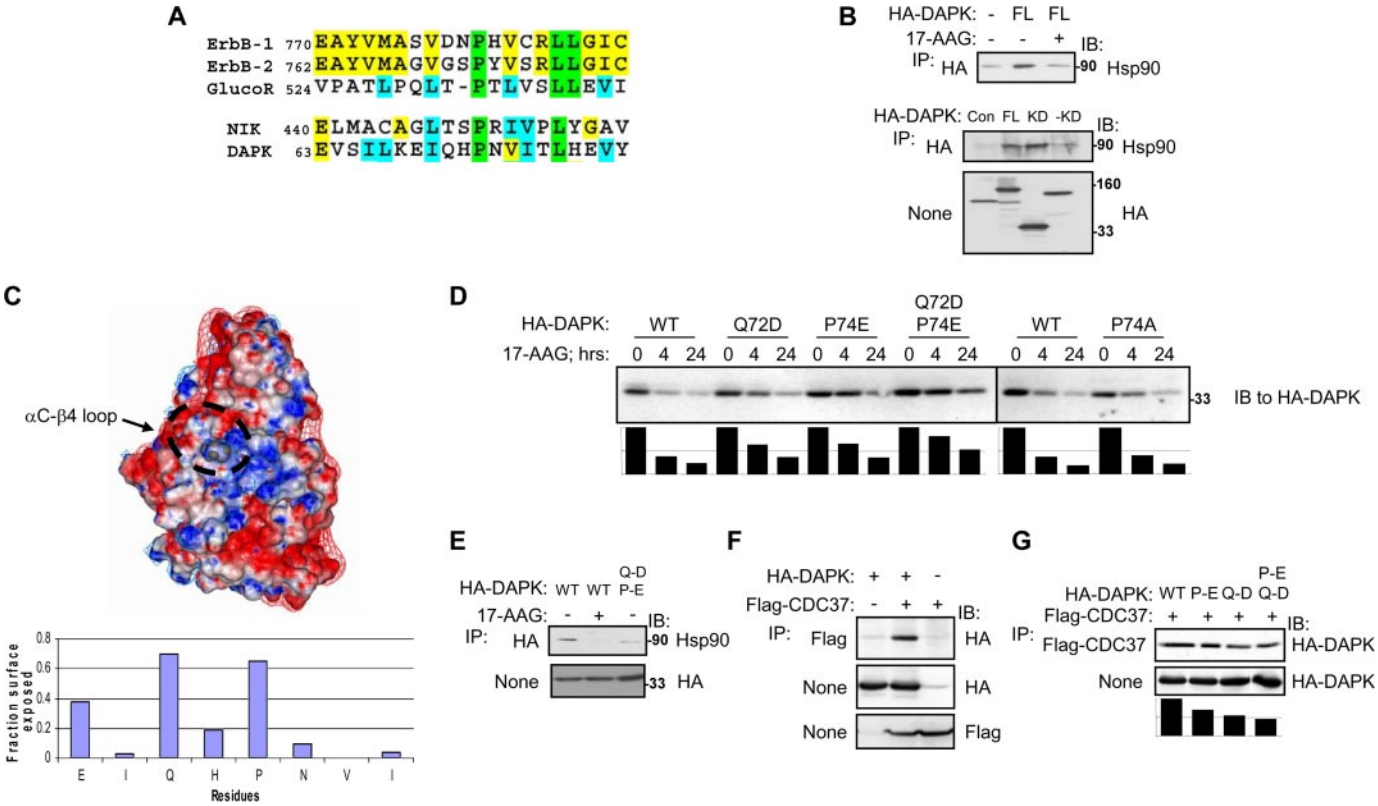

FIGURE 2. **Hsp90 recognizes the novel client protein DAPK through the αC–β4 loop of the kinase.** *A*, sequence alignment of the αC–β4 loop of ErbB-1 and -2 with a region identified as an Hsp90 interaction motif within the glucocorticoid receptor (*GlucoR*) (18). Shown *below* are the sequences within the αC–β4 loop of DAPK and NIK. *B*, HEK293T cells were transfected with vectors encoding HA-tagged DAPK. Twenty-four hours after transfection, the cells were treated for 10 min with 17-AAG (1 μM) followed by lysis and immunoprecipitation (*IP*) of DAPK. Co-precipitated Hsp90 was detected by immunoblotting (*IB*) (*top*). HEK293T cells were transfected with vectors encoding HA-tagged DAPK (*WT*), the kinase domain of DAPK in isolation (KD, amino acids 1–280), or a mutant lacking the kinase domain (−KD, amino acids 276–1423). Whole cell extracts were assayed for expression of HA-tagged DAPK (*bottom*). *C*, structure of the kinase domain of DAPK (PDB code 1JKS), demonstrating an overall neutral (*white*)/positive (*blue*) charge on the backside surface of the molecule (*top*). Shown is the fraction surface exposure of residues within the αC–β4 loop of DAPK (*bottom*). *D*, COS7 cells were transfected with vectors encoding the HA-tagged isolated kinase domain of DAPK (*WT*, amino acids 1–280) or the indicated point or double mutants. Twenty-four hours later, the cells were subjected to treatment with 17-AAG (4 or 24 h at 1 μM) followed by lysis (in radioimmune precipitation assay buffer) and immunoblotting for HA-DAPK. The *bar graphs* represent quantification of the immunoblots as a fraction of the initial expression of each kinase mutant. *E*, HEK293T cells were transfected with vectors encoding HA-DAPK either wild type or the double mutant (Q72D/P74E). Twenty-four hours later, the cells were subjected to treatment with 17-AAG (1 μM for 10 min) followed by immunoprecipitation of HA-DAPK and immunoblotting for Hsp90. *F* and *G*, HEK293T cells were transfected with vectors encoding HA-DAPK (in *G*, mutant HA-DAPK forms were expressed as indicated) and FLAG-CDC37. Twenty-four hours later, the cells were lysed followed by immunoprecipitation of FLAG-CDC37 and immunoblotting for HA-DAPK. The *bar graphs* represent quantification of the level of co-immunoprecipitated DAPK as a fraction of the level observed for wild type.

surface exposure of the residues within the loop, as observed for ErbB-1 (Fig. 2*C*). Utilizing the isolated kinase domain of DAPK, we addressed the effect of introducing a negative charge within the αC–β4 loop on the dependence of the kinase upon Hsp90. Replacing either of two surface-exposed amino acids with acidic residues (Q72D or P74E) resulted in reduction in the sensitivity of the kinase to degradation induced by inhibition of Hsp90 (Fig. 2*D*), whereas replacement of the proline with an alanine (P74A) exerted no effect. Combining the negative charges in both positions had a weak additive effect on the disruption of Hsp90 dependence of the kinase (Fig. 2*D*). In addition, the double mutant displayed reduced interactions with the chaperone, as assayed by co-immunoprecipitation (Fig. 2*E*). The capacity of DAPK to interact with CDC37 (Fig. 2*F*) was also sensitive to the introduction of a negative charge within the αC–β4 loop (Fig. 2*G*).

Addressing the regulation of NIK by Hsp90, we followed the degradation of the protein upon treatment of cells with 17-AAG (Fig. 3, *A* and *B*) as well as its interactions with Hsp90 (Fig. 3*C*). These analyses identified NIK as a novel Hsp90 client in line with recent proteomic mapping of interactions within the NFκB pathway (30). Further, introduction of an aspartate within the αC–β4 loop and replacement of the flanking proline with a glutamic acid inhibited 17-AAG-induced degradation of NIK (Fig. 3*B*) and reduced interactions with Hsp90 (Fig. 3*C*). Likewise, we observed stable NIK-CDC37 interactions (Fig. 3*D*), which were disrupted by the introduction of a negative charge within the αC–β4 loop (Fig. 3*E*).

Hsp90 Recognizes a Well Defined Surface Common to Kinase Clients, rather than a Linear Sequence Motif—To gain insight into the mechanism of recognition of client kinases by Hsp90, we expanded our dataset of Hsp90 clients. Utilizing COS7 cells treated with 17-AAG, we examined the degradation of a large number of both closely and distantly related kinases (see summary of our results in the supplemental table). This analysis added the kinases Epha2, Yes, Pyk2, Cdk2, Rsk1, and Msk1 to the list of clients based on their destabilization upon treatment of cells with 17-AAG. The list of non-clients was also expanded, adding the kinases Tec, Erk3, Erk5, Mek5, Mek1, and βPak. Additionally, we compiled available data from the literature relating to the regulation of kinases by Hsp90 and verified the data for >30 additional kinases (see supplemental table). Assuming a common structure-based mechanism, we grouped all kinases for which interactions with Hsp90 or 17-AAG/GA-induced degradation have been reported. In this way, all four ErbB proteins are defined as Hsp90 clients, although they diverge strongly in the extent of regulation by the chaperone (Fig. 1*A*). Summing up all available evidence from the literature and our own data for regulation of mammalian kinases by Hsp90 resulted in a list of 105 kinases (80 Hsp90

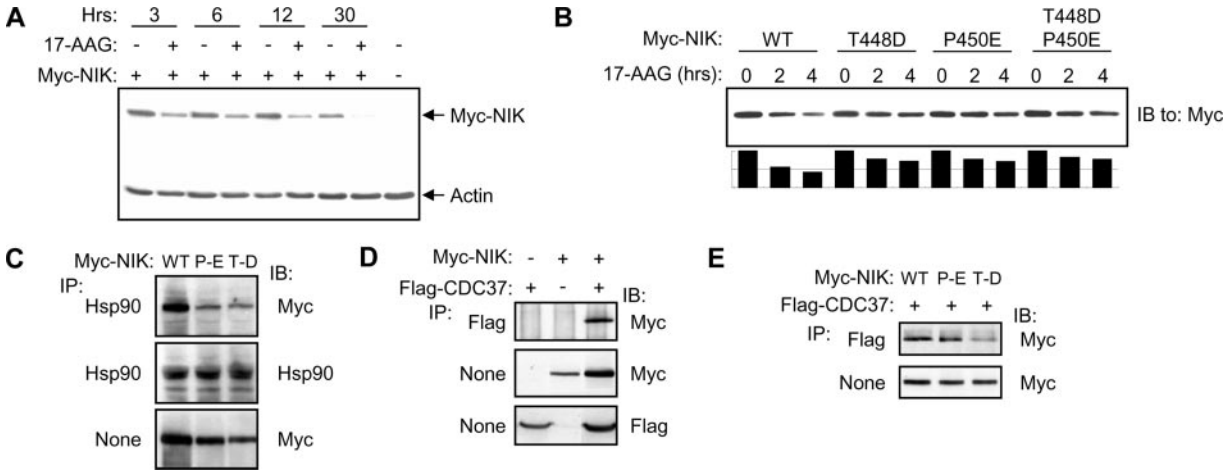

FIGURE 3. **The αC–β4 loop of the novel client protein NIK participates in the interaction with Hsp90.** *A*, COS7 cells were transfected with expression vectors encoding a NIK protein tagged with a Myc peptide. Twenty-four hours after transfection, the cells were treated with 17-AAG (1 μM) for the indicated time intervals (+) or they were left untreated (−). Whole cell lysates were prepared and analyzed for Myc-NIK levels or β-actin as a control. *B*, COS7 cells were transfected with vectors encoding Myc-NIK, either wild type (*WT*) or the indicated mutants. Twenty-four hours after transfection, the cells were treated for the indicated time intervals with 17-AAG (1 μM) followed by lysis and immunoblotting for Myc-NIK. The *bar graphs* represent quantification of the immunoblots as a fraction of the initial expression of each kinase mutant. *C*, HEK293T cells were transfected with expression vectors encoding Myc-NIK or the indicated mutants of NIK. Twenty-four hours after transfection, the cells were lysed followed by immunoprecipitation (*IP*) for Hsp90 and analysis of interactions with Myc-NIK by immunoblotting (*IB*). *D*, HEK293T cells were transfected with vectors encoding Myc-NIK and FLAG-CDC37. Twenty-four hours later, the cells were lysed followed by immunoprecipitation of FLAG-CDC37 and immunoblotting for Myc-NIK. *E*, HEK293T cells were transfected with vectors encoding Myc-NIK (wild type or the indicated mutant forms) and FLAG-CDC37. Twenty-four hours later, the cells were lysed followed by immunoprecipitation of FLAG-CDC37 and immunoblotting for Myc-NIK.

clients, 25 non-clients; see supplemental table), which was mapped on a tree based on sequence homology (Fig. 4) (adapted from Ref. 31). Interestingly, most Hsp90 clients (Fig. 4, *gray ovals*) are found in the families of tyrosine kinases and the related tyrosine kinase-like, in which non-client kinases are rarely observed. In contrast, non-clients (Fig. 4, *black boxes*) are more abundant in several groups of serine/threonine-specific kinases (*e.g.* CMGC, AGC, and STE). It is also interesting to examine the relationship of surface charge within the region of the αC–β4 loop to Hsp90 dependence for kinases with known structures. In a majority of cases (16 of 22), client kinases display an overall neutral or positive charge within the vicinity of the αC–β4 loop. In contrast, the majority of non-clients whose structures were analyzed (5 of 6) displayed an overall negative charge within this same region (data not shown).

We next addressed the potential of defining a consensus sequence for the Hsp90 recognition motif. A profile of Hsp90 client kinases was made from local ungapped block alignments of αC–β4 loop sequences (13 amino acids; MAGVGSPYVSRLLG in ErbB-2) of 73 Hsp90 client kinases, which aligned without gaps. In addition, a non-client profile was made from the αC–β4 loop sequences of 17 non-clients (see supplemental table for sequences). Sequence logos demonstrate the amino acid distribution at each position in these profiles (Fig. 5*B*). The profiles were compared with each other using the LAMA (local alignment of multiple alignments) profile comparison method (32), demonstrating a high similarity of the profiles (data not shown). To further test the validity of the conclusion that there are no significant sequence differences between the profile for Hsp90 clients and non-clients, several additional tests were undertaken. Eight client kinase profiles were created, each excluding one of the kinase families, and each of these profiles was compared with the loop sequences removed from it. The score distributions of these comparisons were not different from comparisons between the profiles of clients and non-clients or from comparisons to a profile created from the loop sequences of all human kinases (518 kinases) (Ref. 31 and data not shown). Taken together, this analysis could not distinguish between sequences of the αC–β4 loop from Hsp90 clients or non-clients. Thus, although the αC–β4 loop is crucial for defining interactions with Hsp90 (Figs. 1–3), recognition of kinases by Hsp90 does not depend on the sequence motifs within this region. Rather, recognition by the chaperone is most likely based on the surface characteristics of the kinase within this region, as defined by the contribution of adjacent residues in the tertiary structure.

Functional Selectivity in Hsp90 Interactions—Addressing the functional selectivity of Hsp90 within a kinase cascade, we focused on the four linear mammalian MAPK cascades (Fig. 6*A*) as well as on the PI3K pathway (Fig. 6*B*). The functional organization of the MAPK and PI3K pathways is markedly different. MAPK cascades integrate input from diverse sources, including stress and activation of surface receptors through to the level of the MAP3K (MAP kinase kinase kinase, e.g. Raf), whereas at the MAP2K-MAPK level, signaling is funneled through a confined channel and no cross-talk occurs between kinase cascades (33). In contrast, the organization of the PI3K pathway is such that it is intersected by other signaling cascades at every level throughout the pathway, receiving inputs that modulate its activity (34, 35). Degradation of endogenous kinases was addressed following treatment of COS7 cells with 17-AAG and the data presented according to the corresponding kinase cascade. Relating to the MAPK cascades, Hsp90 clients are abundant at the MAP3K level, as demonstrated for Raf-1, Mlk3 (Fig. 6*A*), and NIK (Fig. 3), as well as evidence found in the literature for Mos, B-Raf, Ask1, Zak, and Tak-1 (for references, see supplemental table). MEKK3 was an exception to the rule, as this MAP3K appeared to be independent of regulation by Hsp90. In contrast, the layers of MAP2Ks and MAPKs are independent of Hsp90 regulation, regardless of their assignment to specific cascades (Fig. 6*A*). In line with this general conclusion, it has been reported that Mlk3 is subject to regulation by Hsp90, but neither downstream kinase, namely MKK4/7 and JNK, serves as a client (36). Similar observations have been made regarding Raf-1 and the downstream MEK-ERK cascade (37). In contrast to the MAPK cascades, Hsp90 dependence is observed throughout the PI3K-AKT cascade (Fig. 6*B*) (38), consistent with the different functional organization of the pathway, in which every level is subject to a variety of inputs and regulatory interactions. Addressing the question of whether the kinases we defined as non-clients are truly independent of Hsp90 also during their synthesis, we carried out pulse-chase experiments on ErbB-2 and the Hsp90-insensitive kinase JNK in the presence or absence of 17-AAG (Fig. 6*C*). Cells were pulse-labeled for 30 min followed by a 1–3-h chase

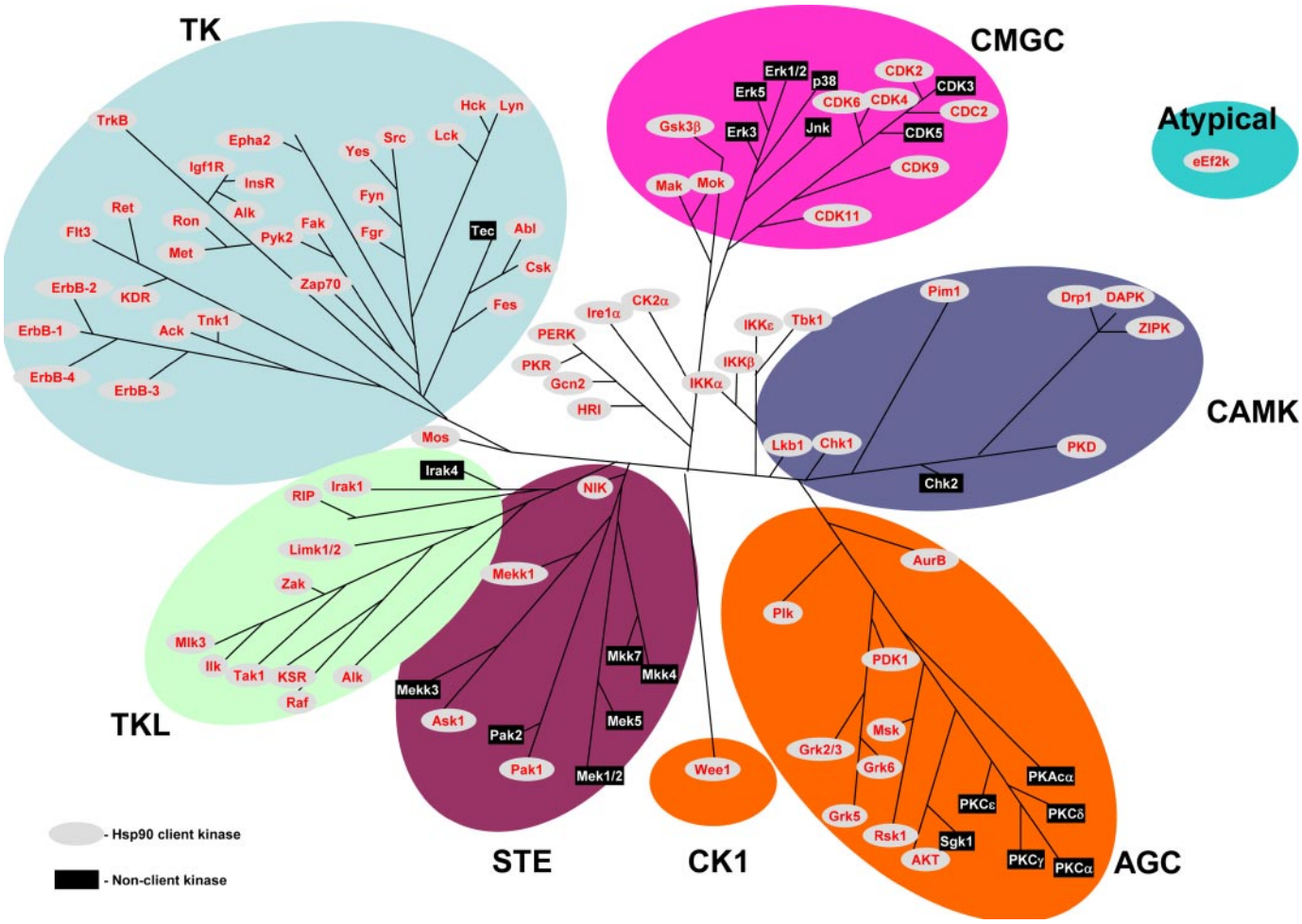

FIGURE 4. **Diversity of established Hsp90 clients within the human kinome.** Shown is a scheme demonstrating the evolutionary relationships and subgroups of protein kinases included in the human kinome. Hsp90 client kinases are represented by *red letters* on an *elliptical gray background*, whereas non-clients appear in *white letters* on a *rectangular black background*. The overall structure of the scheme was based on a previously published analysis of the human kinome (31).

A

Kinase Family	TK	TKL	CAMK	CMGC	AGC	CK1	STE	Other	Atypical	Total
Clients	28	12	7	9	8	1	4	10	1	80
Non-clients	1	2	1	8	6	0	7	0	0	25
Total	29	14	8	17	14	1	11	10	1	105
Total in group	90	43	74	61	63	12	47	83	45	518

B

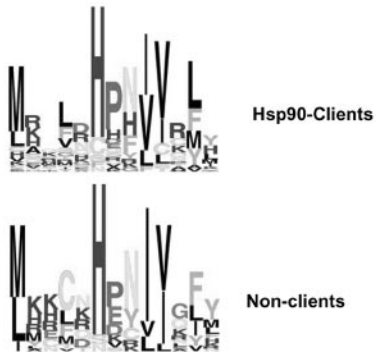

FIGURE 5. **Distribution of Hsp90 clients within kinase families and analysis of the αC–β4 loop sequence.** *A*, tabulation of the diversity of Hsp90 clientele according to kinase families. The data presented is based on our observations for 44 kinases of the 105 kinases addressed, whereas the grouping of the remaining kinases is based on data available in the literature (see supplemental table and references therein). *B*, sequence logos (53) based on the ungapped block alignments of αC–β4 loop regions (13 amino acids) of Hsp90 client kinases (constructed from the sequences of 73 kinases) in contrast to non-client kinases (constructed from the sequences of 17 kinases).

period. The results of these experiments indicate that 17-AAG reduces the accumulation of ErbB-2 and induces degradation of both the mature and immature forms of the kinase, consistent with previous publications (14). In contrast, the MAPK JNK was insensitive to inhibition of Hsp90 during its synthesis and the initial hours following synthesis (Fig. 6*C*), consistent with complete lack of dependence on Hsp90. Interestingly, similar results were obtained by Yun and Matts (39) as to the Hsp90 independence of newly synthesized c-Src in C2C12 cells.

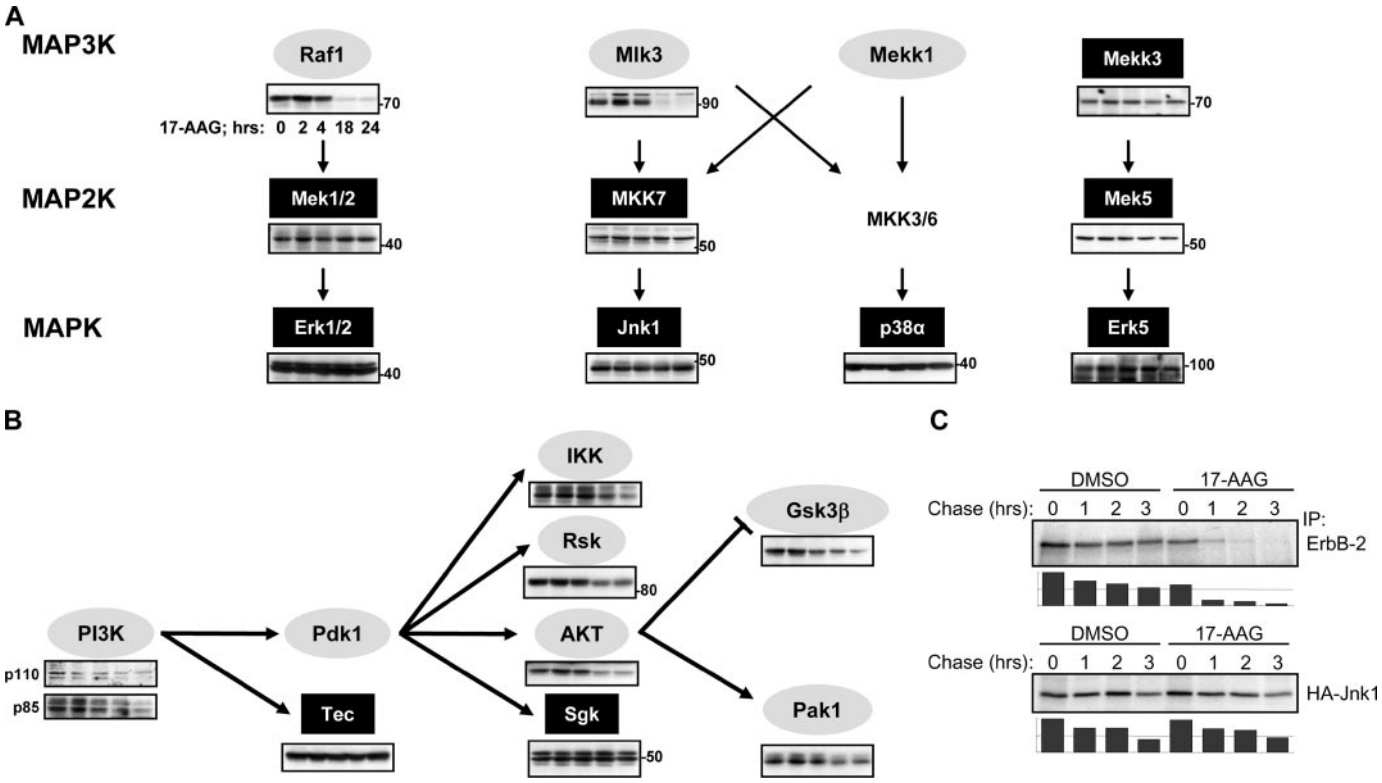

FIGURE 6. **Selective interactions of Hsp90 with components of kinase cascades.** COS7 cells were treated with 17-AAG for increasing time intervals (2, 4, 18, or 24 h at 1 μM) followed by cell lysis and immunoblotting for the indicated proteins. The four MAPK cascades (*A*) are represented as well as the PI3K pathway (*B*). Kinase clients are marked in *gray ovals* and non-clients in *black squares*. *C*, COS7 cells were transfected with expression vectors encoding ErbB-2 or HA-tagged Jnk. Thirty-six hours after transfection, the cells were subjected to amino acid starvation for 4.5 h followed by a pulse of ^{35}S-labeled cysteine and methionine (30 min) in the presence or absence of 17-AAG (1 μM). The cells were then returned to full growth medium for the indicated times ("chase period"), followed by lysis in radioimmune precipitation assay buffer and immunoprecipitation (*IP*) for ErbB-2 or HA-JNK. Following SDS-PAGE, the gels were dried and exposed to film for 4–7 days. The *bar graphs* represent quantification of the radiograms as a fraction of the initial labeling (time 0 in the presence of Me_2SO (*DMSO*)).

DISCUSSION

Structural Selectivity of Hsp90 toward Kinases—Steroid hormone receptors and protein kinases are two major groups of Hsp90 clients, and studies on their interaction with Hsp90 converged on structurally related, but distinct sequence motifs participating in chaperone recognition. Analysis of a 7-amino-acid motif on the glucocorticoid receptor, which is implicated in mediating interactions with Hsp90 (18), demonstrated that the presence of this sequence motif, located on an α-helix in the context of a hydrophobic hinge, is important for chaperone recognition (40). Another major contribution to the understanding of the basis of Hsp90 interactions with clients has come from studies on Lck (19, 20), a Src family member. Although Hsp90 itself bears the potential to interact with multiple discrete regions within the kinase domain of Lck, the interaction of CDC37 is more selective. The primary determinants recognized by CDC37 are the αC helix and part of its adjoining loop connection to the β4-strand. This suggests that CDC37 functions to direct Hsp90 to the appropriate interaction site, consistent with its previously suggested role as a kinase-specific co-chaperone (17). Also in line are deletion analyses, which map Hsp90 interactions to the kinase domains of PDK1 (41), DAPK (Fig. 2*B*), and ErbB-2 (15), as well as studies that narrowed the site to the αC–β4 loop within the amino-terminal lobe of the kinase domain of ErbB-2 (10, 21, 22).

The presence of a common surface mediating interactions of phylogenetically diverse kinase clients with Hsp90 was confirmed by our observations with diverse kinase clients, including DAPK (a CAMK kinase) (Fig. 2) and NIK (a STE kinase) (Fig. 3), demonstrating that a common surface mediates recognition by Hsp90. We have further found that an overall neutral/positive surface charge is characteristic of Hsp90 client kinases in the putative region of interaction. On the other hand, many non-Hsp90-dependent kinases appear to have acquired a negative surface charge within this region, suggesting that a negative charge is detrimental to recognition by Hsp90. These results are consistent with recent observations made with ErbB-2 (22). Interestingly, serine phosphorylation of CDC37 within its amino terminus seems essential for its interactions with client proteins (42). This phosphorylation may act as a filter, limiting the interactions of negatively charged kinases with CDC37. An independent observation demonstrated a naturally occurring mutant of Lkb1 (G163D), which results in loss of interactions with CDC37 and Hsp90 (43). The analogous residue on ErbB-1 maps to the surface of the αE helix, immediately beneath the αC–β4 loop, in line with the possibility that this surface mediates interactions with the CDC37-Hsp90 complex and is disrupted by the introduction of a negative charge.

ErbB-2 provides yet additional potential testament to the physiological relevance of regulation by Hsp90. Eleven naturally occurring mutants of ErbB-2 were identified in tumors of non-small cell lung cancer patients, all of which localize to the αC–β4 loop (44). These mutations create insertions in the αC–β4 loop, which are expected to impact on the structure of the loop. Potentially, these mutations allow the kinase to evade regulation by Hsp90, resulting in hyperactivation (10).

A Cryptic Hsp90 Interaction Motif—Along with promoting the maturation of nascent clients and stabilizing their mature forms, Hsp90 helps maintain client kinases in an inactive state, competent for activation (23). The majority of Hsp90 client kinases are subject to regulation only during their maturation ("weak clients", *e.g.* ErbB-1/epidermal

growth factor receptor and Src-family kinases). In contrast, ErbB-2 and mutant forms of ErbB-1 are dependent on the chaperone also for the maintenance of the mature form and are subject to regulation of their activity by the chaperone ("strong clients") (14). Subtle mutations, both within and outside the kinase domain, can transform a weak client into a strong client (10, 14). Examples of mutational enhancement of Hsp90 regulation have been documented for active forms of Src-like kinases created by a truncation of the SH2 domain or a mutation of the SH2-binding tyrosine residue (45). In the inactive state of the kinase, the intramolecular knot formed by the SH2 and SH3 domains folds them on the backside of the kinase domain, overlaying the αC–β4 loop (46). Likewise, activating mutations within the kinase domain confer Hsp90 dependence to the insulin receptor (47). Additional cases described are Zap70 (48), c-Abl (49), and Plk (50). Taken together, these examples suggest that recognition of kinases by Hsp90 is defined by the exposure of a cryptic determinant, which is normally buried in the quaternary structure of the kinase. This view is consistent with the observations reported here that recognition by Hsp90 is dependent on exposed features of the kinase (Figs. 1–3) rather than on a linear sequence motif (Fig. 5*B* and data not shown).

Functional Selectivity—Mapping the distribution of 105 human kinases (Fig. 5, *B* and *C*; see also supplemental table), we observed that a large proportion of tyrosine kinases and tyrosine-like kinases (40 of the 43 kinases examined) are subject to regulation by Hsp90. In contrast, within the groups of CAMK, CMGC, AGC, CK1, and STE kinases, there is an almost equal number of clients and non-clients (29 clients, 22 non-clients) (Fig. 5*A*). This distribution suggests a preference for Hsp90 to recognize the fold and surface of tyrosine kinases in contrast to serine/threonine kinases. Another emerging pattern is a preference for signaling hubs, as exemplified through the analysis of MAPKs (Fig. 6). From our analysis of the four mammalian MAPK pathways, it appears that most kinases within the MAP3K layer are subject to regulation by Hsp90, whereas the MAP2K and MAPK layers are independent of chaperoning. In principle, the MAP3K layer integrates signals from different sources, leading to the activation of a specific pathway. In contrast, MAP2K and MAPK layers within each cascade act as an insulated amplifier, delivering a precise signal (51). We suggest that the differential regulation by Hsp90 confers an additional level of regulation at nodes in which there is convergence of signaling pathways, and decisions are made regarding specificity of activation, whereas the linear conductance paths of MAPKK-MAPK can be exempt from such regulation. Possibly, Hsp90 acts to regulate the specificity of activation of signaling pathways by regulating the potential of kinases to interact with each other, as in the case of ErbB receptors (10), or with modulatory proteins, as in the case of CDKs (52). In contrast to the MAPK pathways, the PI3K-AKT pathway is subject to regulation by Hsp90 throughout the pathway (38). The fact that the MEK5 activating kinase MEKK3 is not regulated by Hsp90 may suggest that, in contrast to other MAPK cascades, the Erk5/BMK cascade is subject to little cross-talk from other pathways, even at the level of the MAP3K. The functional selectivity suggested for Hsp90 is also consistent with the organization of the PI3K pathway, in which input is received at each level and the pathway is not organized as a linear cascade but rather as a more intricate lattice (34, 35).

In summary, our results propose a modified view of the mechanism of recognition of client proteins by the Hsp90 chaperone machine. In this view, the Hsp90 complex displays a preference to a specific surface on client proteins (the αC–β4 loop region in the case of kinase clients), whereas selectivity is defined by the surface charge on the client protein within this region. Hsp90 clients will boast an overall positive or neutral charge within this region, whereas proteins exempt from chaperone regulation will bear a negative charge. As interaction with this surface can be subject to steric obstruction, the capacity of a given client to interact with Hsp90 is dependent upon the intra- or intermolecular interactions of the client modulating the exposure of the recognition motif.

Acknowledgments—We thank Maxim Shatsky and Prof. Rony Seger for helpful discussion.

REFERENCES

1. Nollen, E. A., and Morimoto, R. I. (2002) *J. Cell Sci.* **115,** 2809–2816
2. Neckers, L., and Ivy, S. P. (2003) *Curr. Opin. Oncol.* **15,** 419–424
3. Pratt, W. B., and Toft, D. O. (2003) *Exp. Biol. Med.* (*Maywood*) **228,** 111–133
4. Millson, S. H., Truman, A. W., King, V., Prodromou, C., Pearl, L. H., and Piper, P. W. (2005) *Eukaryotic Cell* **4,** 849–860
5. Zhao, R., Davey, M., Hsu, Y. C., Kaplanek, P., Tong, A., Parsons, A. B., Krogan, N., Cagney, G., Mai, D., Greenblatt, J., Boone, C., Emili, A., and Houry, W. A. (2005) *Cell* **120,** 715–727
6. Zhang, H., and Burrows, F. (2004) *J. Mol. Med.* **82,** 488–499
7. Richter, K., and Buchner, J. (2001) *J. Cell. Physiol.* **188,** 281–290
8. Brugge, J. S., Darrow, D., Lipsich, L. A., and Yonemoto, W. (1983) *Prog. Clin. Biol. Res.* **119,** 135–147
9. Courtneidge, S. A., and Bishop, J. M. (1982) *Proc. Natl. Acad. Sci. U. S. A.* **79,** 7117–7121
10. Citri, A., Gan, J., Mosesson, Y., Vereb, G., Szollosi, J., and Yarden, Y. (2004) *EMBO Rep.* **5,** 1165–1170
11. Donze, O., Abbas-Terki, T., and Picard, D. (2001) *EMBO J.* **20,** 3771–3780
12. Stepanova, L., Leng, X., Parker, S. B., and Harper, J. W. (1996) *Genes Dev.* **10,** 1491–1502
13. Bijlmakers, M. J., and Marsh, M. (2000) *Mol. Biol. Cell* **11,** 1585–1595
14. Citri, A., Alroy, I., Lavi, S., Rubin, C., Xu, W., Grammatikakis, N., Patterson, C., Neckers, L., Fry, D. W., and Yarden, Y. (2002) *EMBO J.* **21,** 2407–2417
15. Xu, W., Mimnaugh, E., Rosser, M. F., Nicchitta, C., Marcu, M., Yarden, Y., and Neckers, L. (2001) *J. Biol. Chem.* **276,** 3702–3708
16. Smith, D. F. (1998) *Biol. Chem.* **379,** 283–288
17. Riggs, D., Cox, M., Cheung-Flynn, J., Prapapanich, V., Carrigan, P., and Smith, D. (2004) *Crit. Rev. Biochem. Mol. Biol.* **39,** 279–295
18. Xu, M., Dittmar, K. D., Giannoukos, G., Pratt, W. B., and Simons, S. S., Jr. (1998) *J. Biol. Chem.* **273,** 13918–13924
19. Prince, T., and Matts, R. L. (2004) *J. Biol. Chem.* **279,** 39975–39981
20. Scroggins, B. T., Prince, T., Shao, J., Uma, S., Huang, W., Guo, Y., Yun, B. G., Hedman, K., Matts, R. L., and Hartson, S. D. (2003) *Biochemistry* **42,** 12550–12561
21. Tikhomirov, O., and Carpenter, G. (2003) *Cancer Res.* **63,** 39–43
22. Xu, W., Yuan, X., Xiang, Z., Mimnaugh, E., Marcu, M., and Neckers, L. (2005) *Nat. Struct. Mol. Biol.* **12,** 120–126
23. Citri, A., Kochupurakkal, B. S., and Yarden, Y. (2004) *Cell Cycle* **3,** 51–60
24. Berman, H. M., Westbrook, J., Feng, Z., Gilliland, G., Bhat, T. N., Weissig, H., Shindyalov, I. N., and Bourne, P. E. (2000) *Nucleic Acids Res.* **28,** 235–242
25. Stamos, J., Sliwkowski, M. X., and Eigenbrot, C. (2002) *J. Biol. Chem.* **277,** 46265–46272
26. Gilson, M. K., and Honig, B. H. (1987) *Nature* **330,** 84–86
27. Tikhomirov, O., and Carpenter, G. (2000) *J. Biol. Chem.* **275,** 26625–26631
28. Zheng, F. F., Kuduk, S. D., Chiosis, G., Munster, P. N., Sepp-Lorenzino, L., Danishefsky, S. J., and Rosen, N. (2000) *Cancer Res.* **60,** 2090–2094
29. Giannoukos, G., Silverstein, A. M., Pratt, W. B., and Simons, S. S., Jr. (1999) *J. Biol. Chem.* **274,** 36527–36536
30. Bouwmeester, T., Bauch, A., Ruffner, H., Angrand, P. O., Bergamini, G., Croughton, K., Cruciat, C., Eberhard, D., Gagneur, J., Ghidelli, S., Hopf, C., Huhse, B., Mangano, R., Michon, A. M., Schirle, M., Schlegl, J., Schwab, M., Stein, M. A., Bauer, A., Casari, G., Drewes, G., Gavin, A. C., Jackson, D. B., Joberty, G., Neubauer, G., Rick, J., Kuster, B., and Superti-Furga, G. (2004) *Nat. Cell Biol.* **6,** 97–105
31. Manning, G., Whyte, D. B., Martinez, R., Hunter, T., and Sudarsanam, S. (2002) *Science* **298,** 1912–1934
32. Pietrokovski, S. (1996) *Nucleic Acids Res.* **24,** 3836–3845
33. Chang, L., and Karin, M. (2001) *Nature* **410,** 37–40
34. Altomare, D. A., and Testa, J. R. (2005) *Oncogene* **24,** 7455–7464
35. Cantley, L. C. (2002) *Science* **296,** 1655–1657
36. Zhang, H., Wu, W., Du, Y., Santos, S. J., Conrad, S. E., Watson, J. T., Grammatikakis, N., and Gallo, K. A. (2004) *J. Biol. Chem.* **279,** 19457–19463
37. Schulte, T. W., Blagosklonny, M. V., Romanova, L., Mushinski, J. F., Monia, B. P.,

Johnston, J. F., Nguyen, P., Trepel, J., and Neckers, L. M. (1996) *Mol. Cell. Biol.* **16,** 5839–5845
38. Basso, A. D., Solit, D. B., Chiosis, G., Giri, B., Tsichlis, P., and Rosen, N. (2002) *J. Biol. Chem.* **277,** 39858–39866
39. Yun, B. G., and Matts, R. L. (2005) *Exp. Cell Res.* **307,** 212–223
40. Kaul, S., Murphy, P. J., Chen, J., Brown, L., Pratt, W. B., and Simons, S. S., Jr. (2002) *J. Biol. Chem.* **277,** 36223–36232
41. Fujita, N., Sato, S., Ishida, A., and Tsuruo, T. (2002) *J. Biol. Chem.* **277,** 10346–10353
42. Shao, J., Prince, T., Hartson, S. D., and Matts, R. L. (2003) *J. Biol. Chem.* **278,** 38117–38120
43. Nony, P., Gaude, H., Rossel, M., Fournier, L., Rouault, J. P., and Billaud, M. (2003) *Oncogene* **22,** 9165–9175
44. Shigematsu, H., Takahashi, T., Nomura, M., Majmudar, K., Suzuki, M., Lee, H., Wistuba, II, Fong, K. M., Toyooka, S., Shimizu, N., Fujisawa, T., Minna, J. D., and Gazdar, A. F. (2005) *Cancer Res.* **65,** 1642–1646
45. Hartson, S. D., and Matts, R. L. (1994) *Biochemistry* **33,** 8912–8920
46. Huse, M., and Kuriyan, J. (2002) *Cell* **109,** 275–282
47. Imamura, T., Haruta, T., Takata, Y., Usui, I., Iwata, M., Ishihara, H., Ishiki, M., Ishibashi, O., Ueno, E., Sasaoka, T., and Kobayashi, M. (1998) *J. Biol. Chem.* **273,** 11183–11188
48. Matsuda, S., Suzuki-Fujimoto, T., Minowa, A., Ueno, H., Katamura, K., and Koyasu, S. (1999) *J. Biol. Chem.* **274,** 34515–34518
49. An, W. G., Schulte, T. W., and Neckers, L. M. (2000) *Cell Growth & Differ.* **11,** 355–360
50. Simizu, S., and Osada, H. (2000) *Nat. Cell Biol.* **2,** 852–854
51. Morrison, D. K., and Davis, R. J. (2003) *Annu. Rev. Cell Dev. Biol.* **19,** 91–118
52. Wang, H., Goode, T., Iakova, P., Albrecht, J. H., and Timchenko, N. A. (2002) *EMBO J.* **21,** 930–941
53. Henikoff, S., Henikoff, J. G., Alford, W. J., and Pietrokovski, S. (1995) *Gene* (*Amst.*) **163,** GC17–GC26